The interface between the laminar and turbulent flow regions

Ayumu Inasawa, Seiichiro Izawa, Ao-kui Xiong and Yu Fukunishi
Department of Mechanical Engineering, Tohoku University

ABSTRACT

Breakdown process of the Klebanoff mode and origin of turbulence are experimentally investigated in detail. An acoustic excitation using a 2D roughness attached on the wall are used for T-S wave generation. Piezo-ceramic actuators are used to introduce the Klebanoff mode fluctuation. It is found that another shear layer, in which the spike phenomenon takes place and the turbulence starts, exists between the Λ structures aligned in rows. The spreading of the turbulence along the shear layer induced by the Λ structures is newly found.

Key Words : boundary layer, transition, T-S wave, Klebanoff mode

1. Introduction

It is well known that the transition scenario in a flat plate boundary layer starts from the Tollmien-Schlichting (T-S) wave when the intensity of the free stream turbulence is low. The transition process via the T-S wave has been reported by many researchers[1, 2, 3, 4]. However, how the regularity of the instability mode is lost and the turbulent motion starts at the final stage have been left unanswered. Recently, Bake *et al.*[5] conducted a direct numerical simulation against the flow field mentioned above. In their computation, the initial condition was matched to the experimental data. They reported that the random velocity fluctuation appeared from the near wall region, where the strong velocity gradient was present. However, experimental verifications are still necessary because an extremely high-resolution computation is required everywhere in the boundary layer for this kind of flow computations and the grid points may not be enough.

The purpose of the present study is to investigate how the Klebanoff mode breaks down and the turbulence starts.

2. Experimental setup

The experiment is carried out in the low-turbulence wind tunnel at the Institute of Fluid Science, Tohoku University. The flat plate is made of an aluminum alloy, which in 10 mm thick, 3,200 mm long and 1,000 mm wide. The experimental setup is as shown in Fig. 1. The velocity measurement is performed by a single hot-wire probe with CTA circuit. The 300 realizations are used to obtain the ensemble-averaged information in this study.

In order to excite a T-S wave in the boundary layer, a two-dimensional roughness element made of rigid polyvinyl chloride, which is 30 mm wide and 0.3 mm thick, is attached on the wall. Its downstream edge is at $x = 600$ mm. An acoustic wave is installed from a speaker set upstream of the settling chamber of the wind tunnel. The experimental condition is shown in Tab. 1, where $u_{ac,\mathrm{rms}}$ is the intensity of the 77.8 Hz sound wave. To excite three-dimensional Klebanoff mode waves against the T-S wave, an array of uni-morph piezo-electric actuators is mounted at $x = 820 - 900$ mm, $z = -80 - 80$ mm. Total of eight uni-morph piezo-electoric actuators of 0.3 mm thick, 20 mm wide and 80 mm long are aligned side by side along the spanwise direction. Their downstream edge is at $x = 900$ mm. Each actuator is wired independently so that the operation mode can be controlled merely by changing the computer program[6].

Table 1 Experimental conditions

Free stream velocitey U_∞[m/s]	14.0
Intensity of free stream turbulence Tu[%]	0.03
Frequency of exciteation f_0 [Hz]	77.8
Dimensionless frequency F	37.4×10^{-6}
Sound intensity $u_{ac,\mathrm{rms}}/U_\infty$ [%]	0.19
Sound pressure level SPL [dB]	106
Location of Branch I x_I [mm]	560
Location of Branch II x_{II} [mm]	2380

3. Result and discussion

3.1. Exciteation of the T-S wave

Figure 2 shows the wall-normal profile of the amplitude and phase of the T-S wave at $x = 1,100$ mm, $z = 0$ mm. The amplitude profile shows two peaks at $\eta \approx 1$ and $\eta \approx 5$. The phase shift of approximately 180 degrees can be observed at the η location where the amplitude takes the minimum value, i.e. $\eta = 3.6$. These features are in accordance with those found in a T-S wave. The streamwise wavelength is found to be 60 mm and two dimensionality of the T-S wave is also confirmed.

3.2. Excitation of the oblique wave

Figure 3 shows the contour map of the ensemble-averaged velocity fluctuation at $\eta = 1$ in the $x - z$ plane. Here, one of the driving signals of the actuators is used as the reference. The excitation frequency of the oblique wave is also 77.8 Hz. From Fig. 3, it can be found that the positive and negative velocity fluctuating regions are distributed periodically in both the streamwise and spanwise directions. By measuring the

distance between the positive or the negative fluctuation peaks, it is found that the wave lengths of the oblique wave in the streamwise and spanwise directions are 60 mm and 40 mm, respectively. The ratio between them is 3:2, and which matches the wave angle of the Klebanoff mode[2].

3.3. Klebanoff mode excitation against the T-S wave

Figure 4 shows the mean velocity profile in the spanwise direction at $x = 1,100$ mm, $\eta = 1$. In this case, the excitation phase of the piezo-electoric actuators is 180 degrees shifted from that of T-S wave at $x = 1,100$mm, $y = 1$ mm($\eta = 1$), $z = 30$ mm. It can be observed that relatively low velocity spanwise locations exist at $z \approx$ -10, 30 and 70 mm while the velocities of the regions in between are relatively high. These features represent what is known as the peak and valley structures[2, 7]. From Fig. 4, the spanwise scale of the *peak-valley* structure can be measured as approximately 40 mm, which corresponds to the 2/3 wavelength of the T-S wave. The ratio between the streamwise and the spanwise wavelengths agrees with the Klebanoff mode[2]. Thus, it can be confirmed that the system using an array of piezo-electoric actuators is capable of exciting the Klebanoff mode directly against the T-S wave.

3.4. Breakdown of the Klebanoff mode and the start of turbulence

Figures 5 (I) – (IV) show the maps of ensemble-averaged values of (a) velocity fluctuation u/U_∞, (b) velocity gradient fluctuation du/dy and (c) minimum value of the random component in three different frequency bands shown in (d), (e) and (f), which are the intensity of the random component of (d) low- ($f \leq 150$ Hz), (e) middle- (150Hz $\leq f \leq$ 500 Hz) and (f) high- ($f \geq 500$ Hz) frequencies at the $z = 30$ mm (peak) in the $x-y$ plane. Four different phase locations are shown, and how the lambda structure breaks down and the turbulence starts can be examined. Here, the random component corresponds to the amount the velocity fluctuation is dispersed form the ensemble-averaged value at each phase location, and its intensity denotes the RMS value of the dispersion. It is well known that, in the turbulent flow, the broadband frequency component of the velocity fluctuation can be found. So, it should be rational to use the minimum value of the random component intensity in these three different frequency bands as an indicator of the turbulent region, i.e. the red regions in Figs. 5(I)(c)–5(IV)(c) are defined as a turbulent region in this study.

Figure 5(I) shows the maps at $t/T = 0$. In Fig. 5(I)(b), the strong positive shear layers C and C', which are one period different from one another, can be found. Another positive shear layer B existing in between can also be found. The shear layers C and C' in Fig. 5(I) are created by the lambda vortices excited by the actuators. On the other hand, another shear layer which corresponds to B in Fig. 5(I)(b) is newly found. Hereinafter, the shear layer C and B are referred as a *parent* and *child* shear layers, respectively.

At $t/T = 3/4$, random components of the middle- and high- frequency ranges appear at the *child* shear layer location, which is denoted as B' in Figs. 5(III)(e) and (III)(f). In this region, the inflection point in the velocity profile can be found at $x = 1,175$ mm, $y = 2.8$ mm and the single spike signal is observed in the raw velocity data. It is known that the number of spikes increases as flow goes downstream, i.e. the double spikes at $x = 1,190$ mm and the triple spikes at $x = 1,200$ mm can be clearly observed in this experiment, too. At $x = 1,200$ mm, where the triple spike phenomena is observed, as shown in Fig. 6, the near wall region A becomes turbulent as shown in Fig. 5(I)(c). This result agrees with the previous studies[3, 4]. However the strong shear layer found in the DNS result by Bake[5] can not be observed here. It should be noted that the onset of turbulence takes place upstream of the *parent* shear layer.

The expansion of the turbulent region A along the *parent* shear layer can be found at $t/T = 1/4$, which is denoted as D in Fig. 5(II)(c). The low-frequency component spreads only in the near-wall region (Fig. 5(II)(d)) while the middle- and high-frequency components expand to the outer region of the boundary layer along the *parent* shear layer as shown in Figs. 5(II)(e) and (II)(f).

At this phase $t/T = 1/4$, another low-frequency random motion, which is denoted as C' in Fig. 5(II)(d), is found on the *parent* shear layer. This C' is the same as C, but one cycle later. In this area, the middle-frequency component also appears at $t/T = 1/2$ as shown in Fig. (II)(e). However no high-frequency random component can be found. Also in this region, the lax dip signal whose fluctuation is not sharp compared to the *spikes* can be found at $t/T = 1/2 + nT$, as shown in Fig. 6. It can be found that the low- and middle-frequency component , C' in Fig. 5(III)(d) and (III)(e), is due to the lax dip.

In this study, the spike phenomenon was found only on the *child* shear layer, which eventually leads to the onset of turbulence. This finding contradicts to the previous studies[3, 4] where the spike phenomenon was believed to take place at the *parent* shear layer. However, because the time-traced data were used in the previous studies for analyses, it was difficult to identify the exact location of the spike. The time-and-space-traced data obtained in this study show that in Fig. 6, the spike can be found at $t/T = 1/2 + nT$ which corresponds to

the passing of the *child* shear layer (see Fig. 5(I)(b)), while the lax dip can be found at $t/T = nT$ which corresponds to the passing of the *parent* shear layer (see Fig. 5(III)(b)). So as a conclusion, it should be stated that the spike phenomenon starts not from the *parent* but from the *child* shear layer. It was also newly found that the *parent* shear layer itself is playing an important role in the starting stage of turbulence, as the turbulence spreads along this *parent* shear layer.

4. Concluding remarks

The direct excitation of the Klebanoff mode against the T-S wave, which was excited by a combination of the two-dimensional roughness attached on the wall and the acoustic wave in the free stream, was experimentally attempted using an array of the uni-morph piezo-electoric actuators.

The oblique wave was successfully generated using an array of the piezo-electoric actuators which developed into a peak-valley structure whose streamwise and spanwise ratio corresponded to the Klebanoff mode.

Another lambda-shaped shear layer (*child* shear layer) was found between the lambda vortex (*parent* shear layer) which was originally excited by the piezo-electoric actuators. High-frequency instability known as the spike phenomenon was found to take place at the *child* shear layer. It was also confirmed that at the time the triple spikes appeared on the *child* shear layer, the turbulence started at the upstream end of the parent shear layer in the near-wall region. The phenomenon which the turbulence spreads along the *parents* shear layer was newly found.

References

1) Schlichting H. and Gersten K., "Boundary layer theory 8th edition", springer, (1999), pp.415.
2) Klebanoff P. S. , Tidstrom K. D. and Sargent L. M., "The three-dimensional nature of boundary-layer instability", *J. Fluid Mech.* , **12** (1962), pp.1-34.
3) Nishioka M. and Asai M., "Evolution of Tollmien-Schlichting waves into wall turbulence", *Turbulence and Chaotic Phenomena in Fluids* (ed. T. Tatsumi), (1984), pp.87-92.
4) Kachanov Y. S., "Physical mechanisms of laminar-boundary-layer transition", *Annu. Rev. Fluid Mech.*, **26** (1994), pp.411-482.
5) Bake S., Meyer D. G. W. and Rist U., "Turbulence mechanism in Klebanoff transition: a quantitative comparison of experiment and direct numerical simulation", *J. Fluid Mech.*, **459** (2002), pp.217-243.
6) Fukunishi Y., Izawa S. and Morita K., *Fluid Dyn. Res.*, printing.
7) King R. A. and Breuer K. S., "Oblique transition in a laminar Blasius boundary layer", *J. Fluid Mech.*, **453** (2002), pp.177-200.

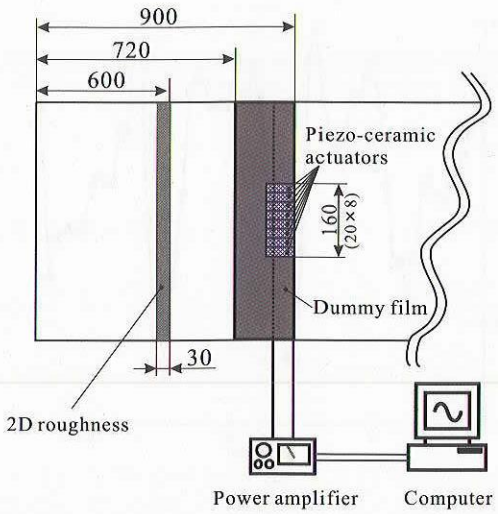

Fig.1 Experimental setup.

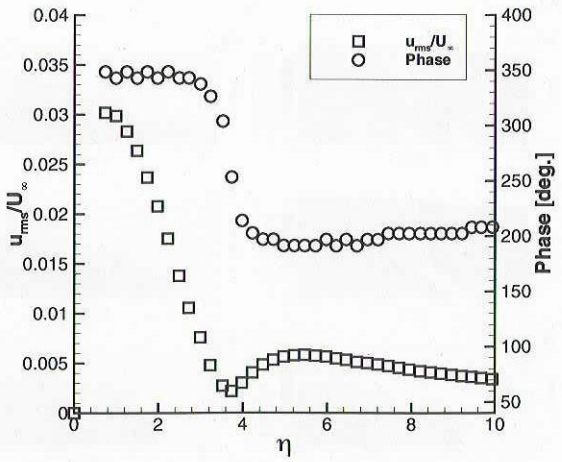

Fig.2 Amplitude and phase profiles of the T-S wav ($x = 1,100$ mm, $z = 0$ mm).

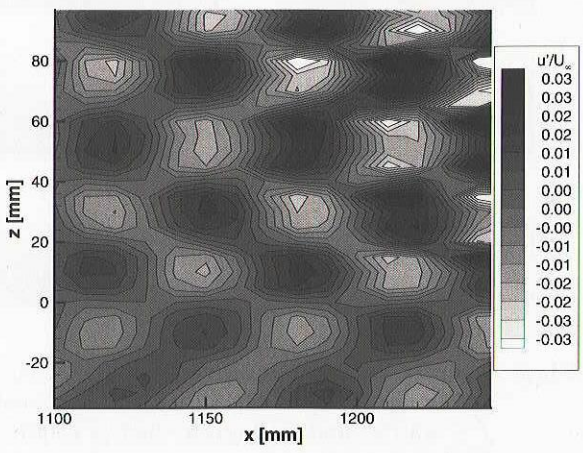

Fig.3 Contour map of ensemble-averaged velocity fluc tuation ($\eta = 1$).

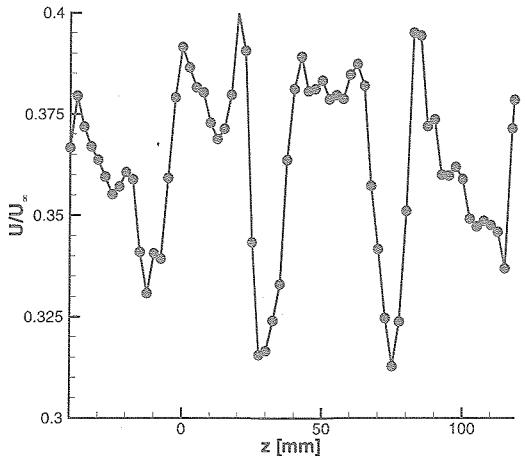

Fig.4 Mean velocity in the spanwise direction ($x = 1,100$mm, $\eta = 1$).

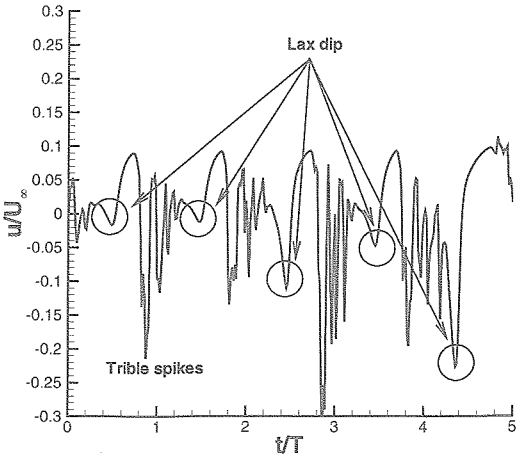

Fig.6 Lax dip in the raw signal of the velocity fluctuation at $x = 1,200$ mm, $y = 3.7$ mm.

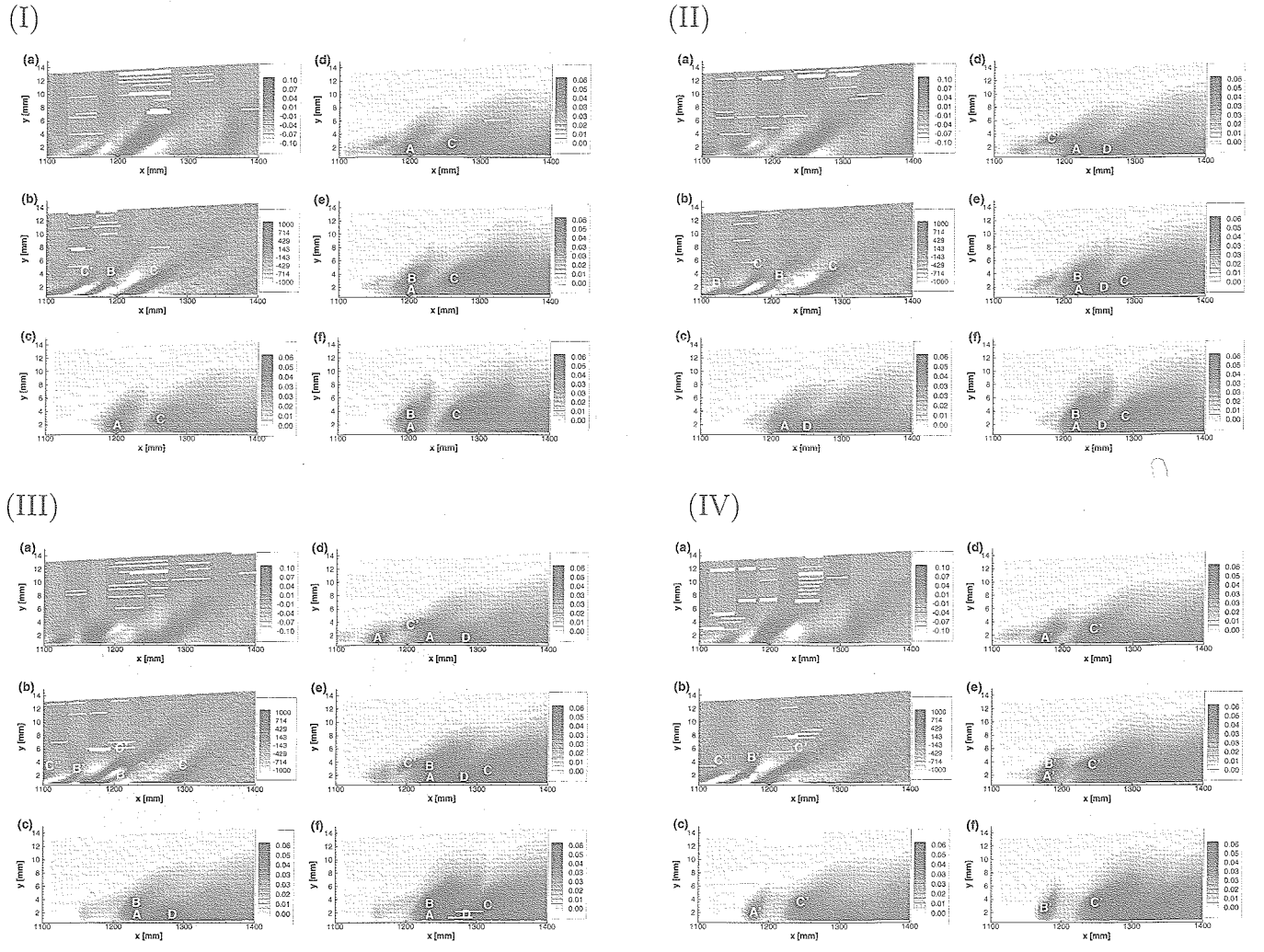

Fig.5 Maps of ensemble-averaged (a) u/U_∞, (b) du/dy and (c) minimum value displayed in (d), (e) and (f), which are the intensity of the random component at (d) low-frequency ($f \leq 150$Hz), (e) middle-frequency ($150\text{Hz} \leq f \leq 500\text{Hz}$) and (f) high-frequency ($500\text{Hz} \leq f$), respectively. (I) $t/T = 0$, (II) $t/T = 1/4$, (II) $t/T = 1/2$ and (IV) $t/T = 3/4$.